Parameters optimization of improved air-assisted orchard sprayer based on RSM and RBF neural network

Qu Feng, Zhang Mingming, Li Xi, Zhang Junxiong*, Liu Jingyun

(College of Engineering, China Agricultural University, Beijing 100083, China)

Abstract: As traditional axial-flow air-assisted orchard sprayer is lack of guidance for the air-assisted spray, it causes droplets easily drift into the air or fall on the ground, which wastes lots of pesticides and cannot satisfy the desired prevention and cure effects. In order to improve spraying performance of the traditional sprayer, linear guide plates were installed above the upper air outlet of the sprayer. Orthogonal tests with mixed levels based on Box-Behnken method were designed. Length and angle of guide plate, air velocity of air outlet, and pressure of pump were opted as the experimental factors. In addition, droplet coverage rate was taken as an evaluation index of spraying. Combined Response Surface Method (RSM) with Computational Fluid Dynamics (CFD), wind field of the improved prayer was simulated, and influences of the simulation wind field on test results were analyzed. RSM model and Radical Basis Function (RBF) Neural Network model were respectively adopted to approximate the relationships and establish the approximate models between the experimental factors and the experimental data. Experimental factors were analyzed and optimized based on different approximate models, and the model of RBF Neural Network was proved to be the better one in the verification tests at different sample heights. In verification tests, at the height of 150 cm, droplet coverage rate and forecast error were 55.06% and 3.5%; at the height of 200 cm, they were 28.13% and 5.2%; at the height of 250 cm, they were 17.01% and 9.2%. The results will provide references for parameters optimization of the improved air-assisted orchard sprayer.

Keywords: air-assisted sprayer, response surface method, approximate model, parameter optimization

Citation: Qu, F., M. M. Zhang, X. Li, J. X. Zhang, and J. Y. Liu. 2017. Parameters optimization of improved air-assisted orchard sprayer based on RSM and RBF neural network. International Agricultural Engineering Journal, 26(3): 64–74.

1 Introduction

Air-assisted sprayer plays an important role in orchard spraying and improvements of its spraying performance have been widely studied and applied for recent years. Researches on spraying characteristics, influence factors, parameters optimization and experimental verification using characters of gas-liquid two-field flow field based on CFD have achieved some results. Most of them were focused on establishing airflow field models (Endalew et al., 2010; Salcedo et al., 2015) and finding out laws of droplet deposition (Qi et al., 2010; Wang et al., 2015) which proved method based on CFD is able to provide effective references. However, because of restricted accuracy of models and complicated atomization principles, method based on CFD cannot completely simulate the real spraying situation. Effects of air-assisted spraying can be affected by multiple factors, such as mass concentration of pesticide (Qiu et al., 2015), wind velocity of fan (Sun et al., 2015; Song et al., 2011), sprayer structure (Song et al., 2013) and so on. Most researches had just considered a single factor during tests and neglected interactions between deferent factors, which can hardly explain the actual influences on spraying effects of each factor. Although combinations of air-assisted sprayer and electrostatic sprayer (Zhou et al., 2016; Wang et al., 2015), automatic target sprayer (Jiang et al., 2016), disc sprayer (Zhou et al., 2015) or directional sprayer (Zhang et al., 2014; Zhang et al., 2016) have provided new methods for improving air-assisted orchard sprayer, there still seldom have studies on wind

Received date: 2017-03-22 **Accepted date:** 2017-08-13

* **Corresponding author: Zhang Junxiong,** Ph.D., Associate Professor of College of Engineering, China Agricultural University, 100083, Beijing, China. Email: cau2007@cau.edu.cn. Tel: (86)10-62737726.

field guidance for circle arranged nozzles of axial-flow sprayer, especially lack units or methods which are able to guide upper airflow of sprayer. Droplets are easy to drift into the air or fall on the ground which leads to huge waste of pesticides is still an urgent problem.

This paper selected the general used axial-flow air-assisted orchard sprayer (Gu et al., 2014) as the study object, whose air intake is axial set and air outlet is circle arranged. A linear guide plate was installed above the upper air outlet of the sprayer to guide wind field of fan. And orthogonal tests with mixed levels based on Box-Behnken method were designed to find out the influences on spraying effects of different factors. The results will provide references for parameters optimization of the improved air-assisted orchard sprayer.

2 Devices and methods

2.1 Test devices

For fruit trees such as apple, pear, peach, pomelo and so on, canopy height about 1.5-2.5 m, bottom height of canopy is about 0.5-1.0 m, row spacing of trees is about 4 m. And spray range of traditional axial-flow air-assisted orchard sprayer covers a sector whose center is the axis of fan, schematic of the range is shown as α which is equal to 240° in Figure 1. There are no crops in the sector area above sprayer during spraying, causing droplets easily drift into the air or fall on the ground, which wastes lots of pesticides and cannot satisfy the desired prevention and cure effects. In order to solve this problem, an improved air-assisted orchard sprayer was designed. Two linear guide plates whose cross section was C shape were symmetrically installed above the upper air outlet of the sprayer to change its flow direction, which was aimed at improving spraying performances.

An improved self-propelled air-assisted orchard sprayer was selected as test devices in this study, and structure of the sprayer is shown in Figure 2. Diameter of the axial-flow fan is 580 mm and its maximum revolving speed is 2700 r/min. At the maximum speed, air velocity of its outlet is 25 m/s+/-0.5 m/s and air volume is 14722 m^3/h. In order to study the influences of guide plate length on spraying quality, two guide plates with different sizes which were 38 cm and 88 cm were designed according to the canopy sizes of different fruit trees. Angle between guide plate and horizontal direction was adjustable from 0 to 90°. Guide plates were installed above the upper air outlet of the fan and the height from ground is about 1 m. Ten orange nozzles (D2) which produced by Tee Jet company were installed around air outlet of the axial-flow fan. The nozzles were all equipped with drip-proof and rotary tip, and their parameters are list as follow: spray angle is 74°, working pressure is 0.5-1.5 MPa, flow is 0.41-0.63 L/min. Both movement and spraying of the sprayer can be remote controlled.

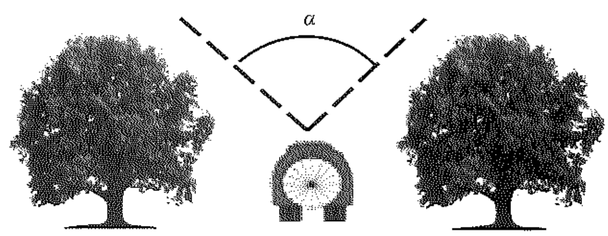

Figure 1 Schematic of spray range

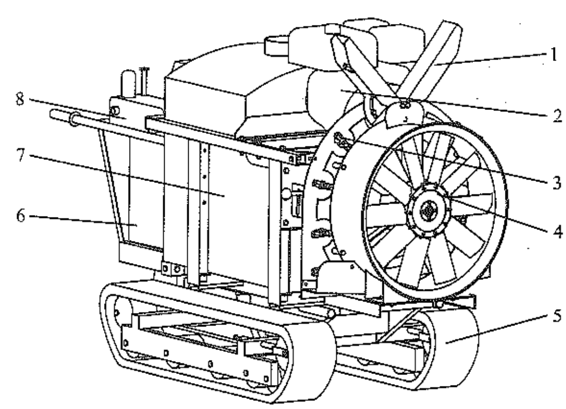

1. Guide plate 2. Fan engine 3. Nozzle 4. Axial-flow fan 5. Moving mechanism 6. Control cabinet 7. Pesticide tank 8. Plungerpump

Figure 2 Structure of self-propelled air-assisted orchard sprayer

2.2 Test design and methods

Operation quality of the improved sprayer was measured based on occupation standard of 'The Operation Quality of Air-assisted Orchard Sprayer' (NY/T992-2006). As structure of axial-flow fan and installation position of nozzles are both symmetrical, tests and simulation based on one side is acceptable and adequate. Instead of real crops, 300 cm height poles were designed as simulated targets according to situation of crops cultivation and structure size of sprayer. Within heights from 150 to 250 cm, three test units were uniformly set as 150, 200 and 250 cm. Every unit had been placed four pieces of water sensitive paper which produced by Syngenta company and its sizes is 2×3 cm. In each unit, two water sensitive papers are horizontally placed, and others are vertically placed. As is shown in Figure 3, all poles were set in a line which was 200 cm far away from the center line of the sprayer, and distance between each pole was 300 cm.

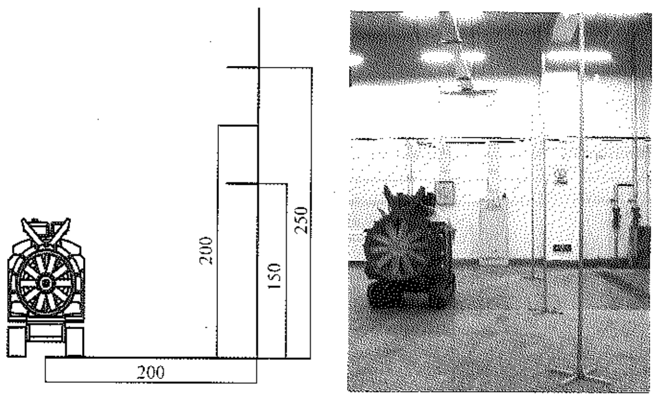

a. Schematic of pole b. Testing site

Figure 3 Spraying test

Orthogonal tests with mixed levels based on Box-Behnken method were designed. Length and angle of guide plate, air velocity of air outlet, and pressure of pump were opted as experimental factors. Levels of each factor are presented in Table 1. In addition, droplet coverage rate was taken as the evaluation index of spraying. There are totally 34 group tests, and the average droplet coverage rate of water sensitive papers at the same height was adapted as final result in every group.

Table 1 Factors and levels table

Levels	Factors			
	A: Angle of guide plate, °	B: Air velocity of fan, m/s	C: Pressure of pump, MPa	D: Length of guide plate, cm
+1	55	25	1.5	88
0	35	20	1.0	-
−1	15	15	0.5	38

When sprayer pass through sampling area, droplets will deposit on water sensitive papers caused by drag force of air flow and become blue spots. After field tests, using industrial camera (Mercury 20) produced by IMAVISION company to collect images of water sensitive papers. As droplet coverage rate is defined as ratio of blue area to total area of water sensitive paper, it is easily to figure out the results by image processing techniques using MATLAB. Images with different droplet coverage rate were shown in Figure 4. Meteorological parameters of tests were also recorded and presented as follows: temperature ranged from 10°C to 17°C, maximum relative humidity was 60%, average wind velocity was under 1.5 m/s and travel speed of sprayer was 0.76 m/s.

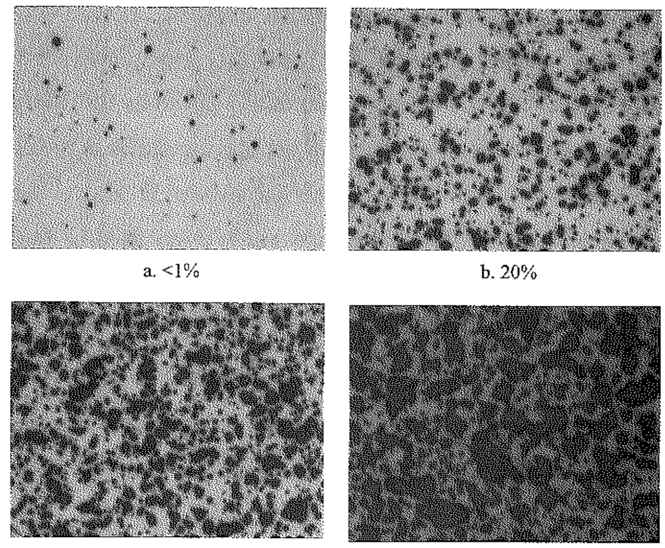

a. <1% b. 20%

c. 40% d. 60%

Figure 4 Images with different droplet coverage rates

3 Results and analysis

3.1 Test results

From the test results presented in Table 2, it is easily to find out that droplet coverage rate decrease with sampling height increase, which is probably caused by changing of airflow filed around the axial-flow fan. In order to confirm this presume, according to methods of reference article (Qi et al., 2010; Wang et al., 2015), airflow filed around the axial-flow fan was simulated using Fluent software. In the simulation, the boundary conditions were set as follow: (1) temperature was 15°C; (2) relative humidity was 45%; (3) gas viscosity was 1.789×10^{-5} Pa·s; (4) the half arc on the left side was set as velocity inlet, which was the airflow inlet; (5) upside and right side of the axial-flow fan were set as free outlet; (6) the left side of the simulation field were set as the symmetry; (7) the other boundaries were set as no-slip wall conditions. Speed fields of different airflow in test areas were figured out through k-ε turbulence model, which are shown in Figure 5. And results indicated that distribution characteristics of different speed fields which are 15, 20 and 25 m/s were similar to each other, only the magnitude were different. So there just gives out partial simulation results which presented in Table 2.

Table 2 Test results

No.	Factors				Droplet coverage rate at different heights, %		
	A: Angle of guide plate, °	B: Air velocity of fan, m/s	C: Pressure of pump, MPa	D: Length of guide plate, cm	150 cm	200 cm	250 cm
1	15	15	1.00	38	18.49	2.38	0.52
2	55	15	1.00	38	30.71	17.80	2.58
3	15	25	1.00	38	10.48	3.17	0.45
4	55	25	1.00	38	11.47	12.71	5.27
5	15	20	0.50	38	11.95	1.86	0.46
6	55	20	0.50	38	28.85	16.80	7.09
7	15	20	1.50	38	20.72	3.66	1.55
8	55	20	1.50	38	33.19	29.62	12.42
9	35	15	0.50	38	36.54	18.10	3.01
10	35	25	0.50	38	30.18	12.67	6.18
11	35	15	1.50	38	58.93	20.75	10.00
12	35	25	1.50	38	25.59	26.56	12.22
13	35	20	1.00	38	22.35	25.27	9.91
14	35	20	1.00	38	22.42	17.13	9.13
15	35	20	1.00	38	24.48	21.52	8.66
16	35	20	1.00	38	20.32	13.83	10.68
17	35	20	1.00	38	22.88	18.74	10.22
18	15	15	1.00	88	12.05	3.29	1.89
19	55	15	1.00	88	38.98	22.43	6.94
20	15	25	1.00	88	36.89	3.39	0.01
21	55	25	1.00	88	32.03	21.11	4.02
22	15	20	0.50	88	27.96	6.57	2.50
23	55	20	0.50	88	48.00	15.28	10.47
24	15	20	1.50	88	26.17	7.28	3.23
25	55	20	1.50	88	38.55	22.57	10.04
26	35	15	0.50	88	47.19	21.31	14.71
27	35	25	0.50	88	48.99	11.48	3.34
28	35	15	1.50	88	44.17	20.08	7.51
29	35	25	1.50	88	38.10	24.37	5.40
30	35	20	1.00	88	36.84	22.19	12.43
31	35	20	1.00	88	40.35	25.60	12.24
32	35	20	1.00	88	32.32	20.06	6.92
33	35	20	1.00	88	36.85	25.78	12.95
34	35	20	1.00	88	39.67	26.01	7.69

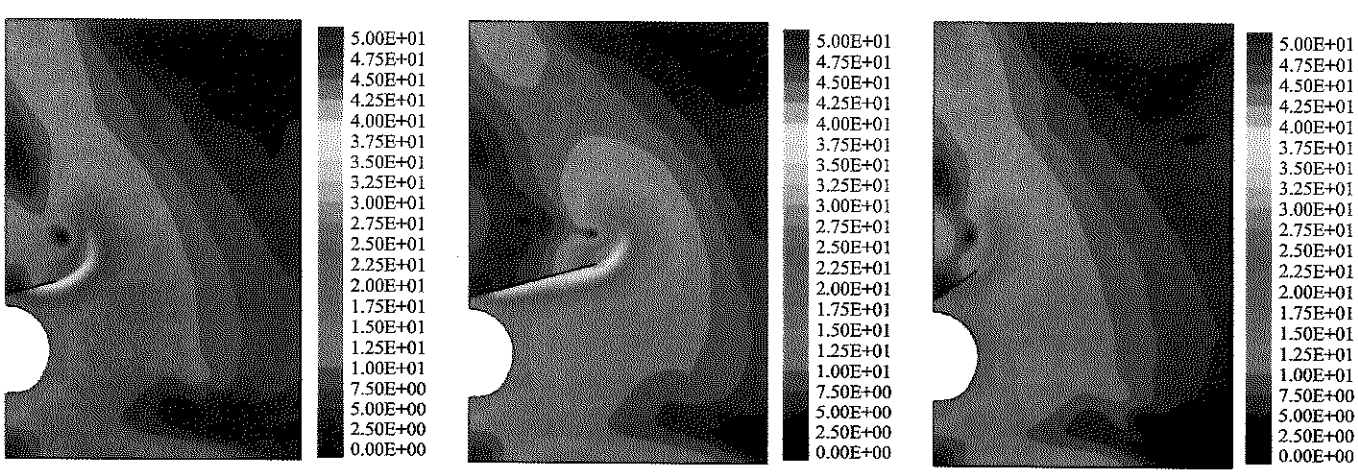

a. A=15°, D=38 cm, v=20 m/s b. A=15°, D=88 cm, v=20 m/s c. A=35°, D=38 cm, v=20 m/s

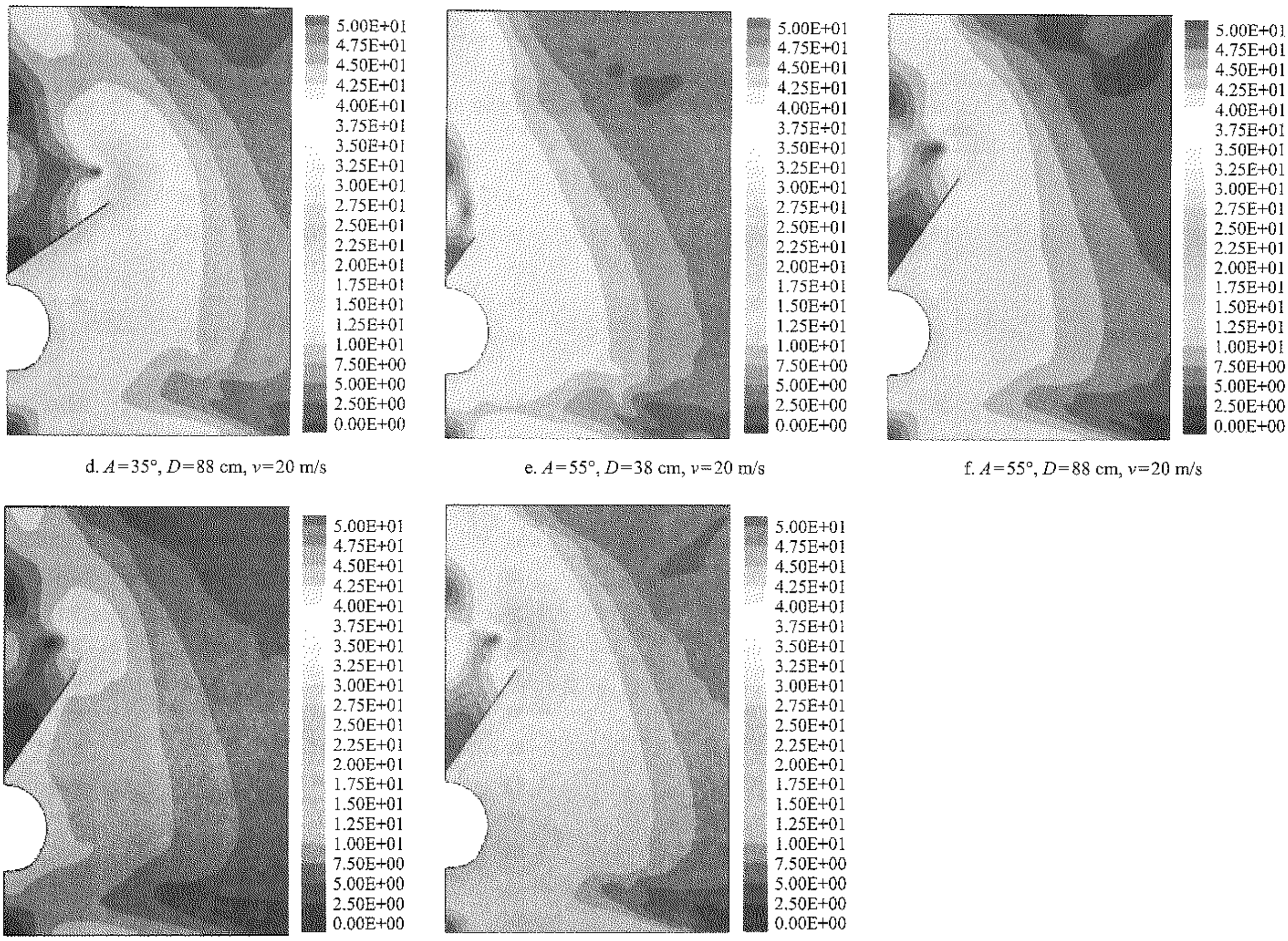

d. A=35°, D=88 cm, v=20 m/s   e. A=55°, D=38 cm, v=20 m/s   f. A=55°, D=88 cm, v=20 m/s

g. A=55°, D=88 cm, v=15 m/s   h. A=55°, D=88 cm, v=25 m/s

Figure 5 Speed field of air flow with different lengths and angles of guide plate

3.2 Analysis of variance (ANOVA)

In consideration of quadratic influences between different factors, it is necessary to analyze the variances of data presented in Table 2. Analysis results had indicated the response relationships between parameters of prayer and different sampling heights which presented in Table 3. Significant degrees of each factor influenced on droplet coverage rate were figured by F test, and the smaller P value is, the more significant influence on droplet coverage rate is. In the vertical plane which was 200 cm away from the center line of axial-flow fan and according to Table 3, it is easily to conclude that: (1) at height of 150 cm, factors of significant influences whose P value is bigger than 0.05 on droplet coverage rate are A, B, D, AB, BC, BD, CD, A^2, C^2, and the other factors are not significant whose P value is smaller than 0.05; (2) at height of 200 cm, significant factors are A, C, D, BC, A^2, B^2; (3) at height of 250 cm, significant factors are A, C, BD, CD, A^2, B^2.

3.3 Influences of each factor on droplet coverage rate

According to P value in Table 3, at height of 150 cm, the sequence of factors, according to significant degree of influences on droplet coverage rate, was D, A, Band C. As pressure of pump had less influence on droplet coverage rate, the droplet coverage rate at this height can be seemed as influencing by interaction of D, A and B. When D was equal to 38 cm and C was at average level which was equal to 1.0 MPa, response surface figure of interaction A with B was shown in Figure 6a. When D was equal to 88 cm and C was at average level, response surface figure of interaction A with B was shown in Figure 6b. Both of them indicated that: (1) with increasing of guide plate angle, droplet coverage rate increased at first and then decreased; (2) when guide plate length was 38 cm, droplet coverage rate decreased with air velocity increasing; (3) when guide plate length was 88 cm, droplet coverage rate increased a little at high air velocity.

Table 3 ANOVA table

Variables	Droplet coverage rate at 150 cm height				Droplet coverage rate at 200 cm height				Droplet coverage rate at 250 cm height			
	SS	DF	F value	P value	SS	DF	F value	P value	SS	DF	F value	P value
Models	37.060	13	19.030	<0.0001	45.570	13	24.120	<0.0001	29.980	13	19.620	<0.0001
A	5.770	1	38.500	<0.0001	24.500	1	168.610	<0.0001	10.480	1	89.190	<0.0001
B	1.390	1	9.270	0.0064	0.120	1	0.840	0.3690	0.420	1	3.590	0.0728
C	0.034	1	0.230	0.6379	2.390	1	16.430	0.0006	0.730	1	6.190	0.0218
D	10.140	1	67.690	<0.0001	0.880	1	6.020	0.0234	0.230	1	1.960	0.1765
AB	2.290	1	15.280	0.0009	0.140	1	0.960	0.3381	0.240	1	2.000	0.1727
AC	0.200	1	1.310	0.2666	0.280	1	1.940	0.1793	0.000	1	0.000	0.9917
AD	0.021	1	0.140	0.7125	0.170	1	1.170	0.2913	0.022	1	0.190	0.6674
BC	0.890	1	5.950	0.0241	1.110	1	7.620	0.0121	0.170	1	1.460	0.2406
BD	4.060	1	27.130	<0.0001	0.009	1	0.060	0.8088	2.280	1	19.370	0.0003
CD	1.340	1	8.920	0.0073	0.120	1	0.840	0.3707	1.160	1	9.900	0.0051
A^2	6.180	1	41.260	<0.0001	14.700	1	101.140	<0.0001	10.160	1	86.440	<0.0001
B^2	0.270	1	1.780	0.1966	0.740	1	5.060	0.0359	3.380	1	28.750	<0.0001
C^2	5.050	1	33.690	<0.0001	0.010	1	0.072	0.7910	0.260	1	2.170	0.1559
Residual	3.000	20			2.910	20			2.350	20		
Lack of Fit	2.620	12	4.650	0.0184	1.610	12	0.830	0.6261	1.420	12	1.020	0.5060
Error	0.380	8			1.290	8			0.930	8		
Total	40.050	33			48.480	33			32.330	33		

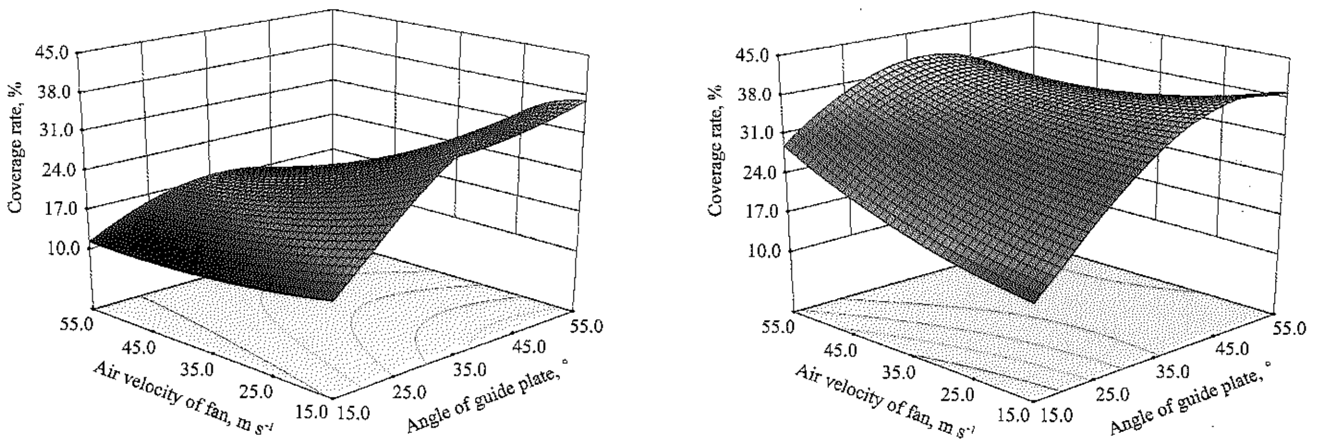

a. C=1.0 MPa, D=38 cm

b. C=1.0 MPa, D=88 cm

Figure 6 Influences of interaction factors on droplet coverage at 150 cm height

Combined with simulation results of Figure 5, it can be concluded that: (1) when guide plate angle was small, droplets fell down to the ground by drag force of air flow and caused low droplet coverage rate; (2) when guide plate angle was too big, droplets drifted upward targets of poles and also caused low droplet coverage rate; (3) when guide plate length increased, airflow field got closer to sampling targets of poles, which was similar to reduce distance between poles and sprayer, so droplet coverage rate increased a little with air velocity increased.

At height of 200 cm, the sequence of factors, according to significant degree of influences on droplet coverage rate, was A, C, D and B. As length of guide plate had less influence on droplet coverage rate, average of guide plate length was selected to analyze the results. According to interaction analysis of different factors, the other factors were correspondingly selected at average level calculated by the software of Design-Expert 8.0.6, and response surface figures were shown in Figure 7. According to the figures, it can be found that: (1) with air velocity increasing, droplet coverage rate change a little, which indicated air velocity of fan had less influence on droplet coverage rate and is in accordance with Table 2; (2) at the height of 200 cm, with increasing of guide plate angle, droplet coverage rate increased at first and then decreased which is same as at height of 150 cm; (3) droplet coverage rate increased with pump pressure increasing, which caused by increasing of spraying flow.

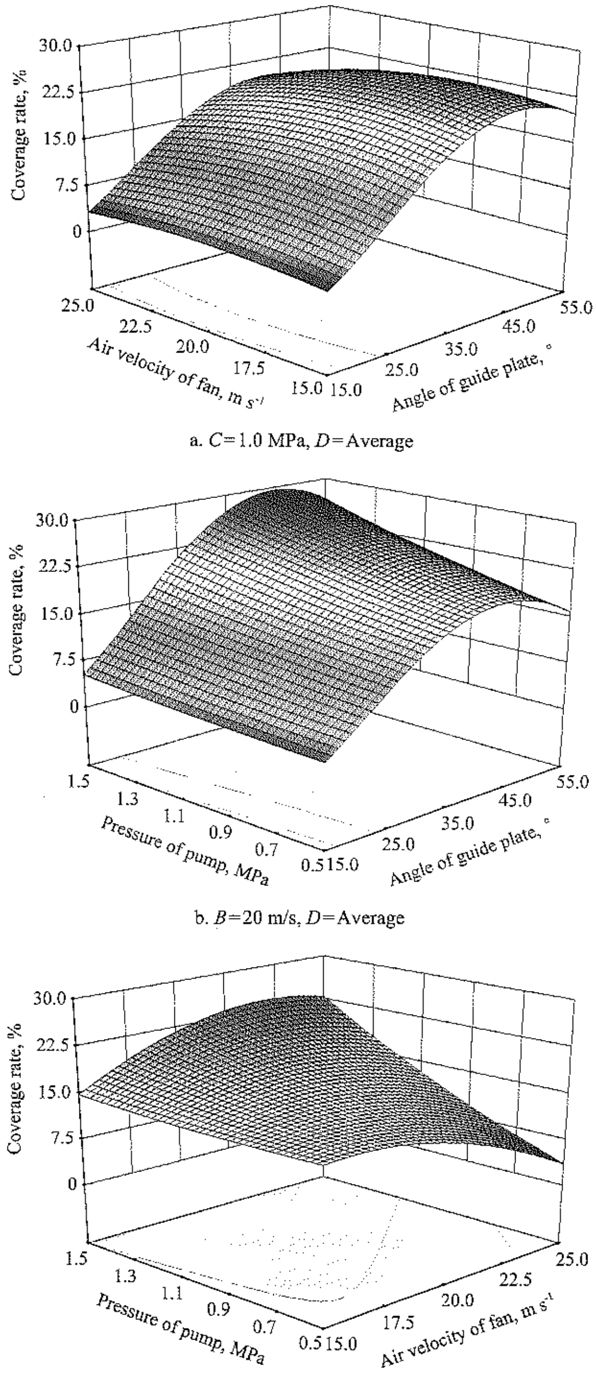

a. C=1.0 MPa, D=Average

b. B=20 m/s, D=Average

c. A=35°, D=Average

Figure 7 Influences of interaction factors on droplet coverage at 200 cm height

At the height of 250 cm, the sequence of factors, according to significant degree of influences on droplet coverage rate, was A, C, B and D. Also, guide plate length was selected as average value, and according to interaction analysis of different factors, the other factors were correspondingly selected at average level, response surface figures were shown in Figure 8. According to the figures, we can find that: (1) at the height of 250 cm, the factor of most significant influence on droplet coverage rate was guide plate angle which is same as height of 150 cm and 200 cm; (2) droplet coverage rate increased with pump pressure increasing, which also caused by increasing of spraying flow; (3) with increasing of air velocity, droplet coverage rate increased at first and then decreased, which was caused by straight movement more than deposition movement of droplets.

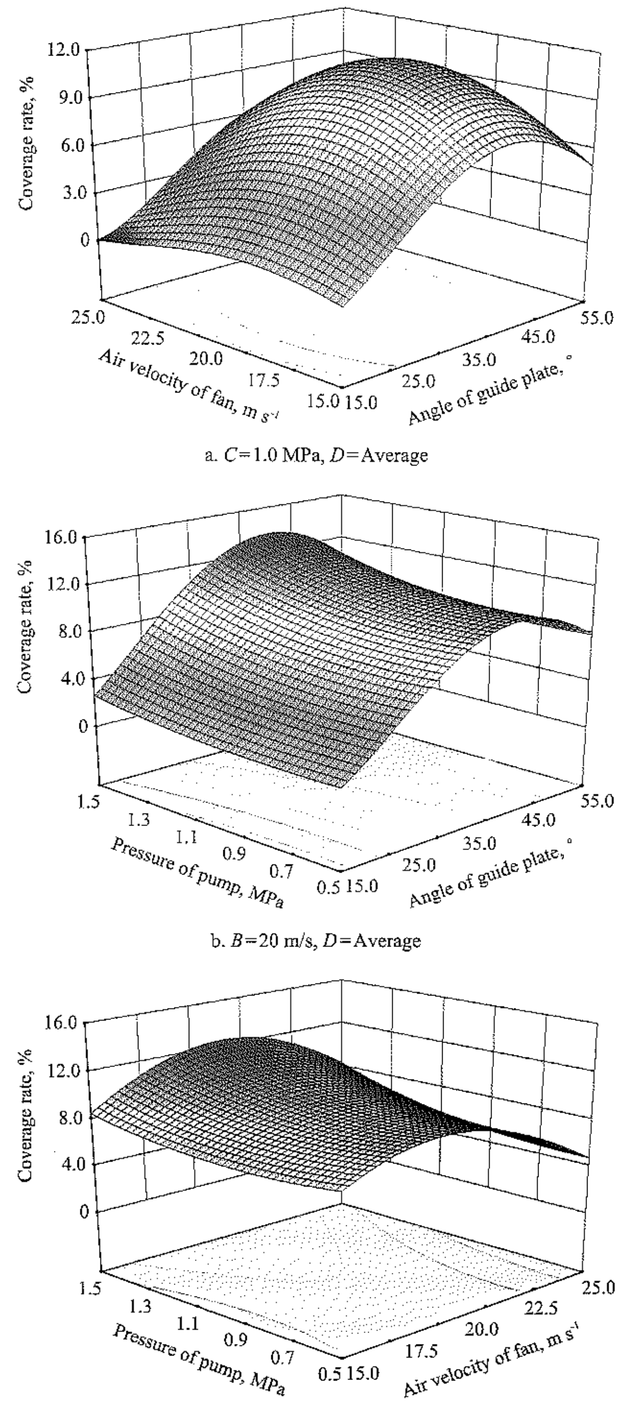

a. C=1.0 MPa, D=Average

b. B=20 m/s, D=Average

c. A=35°, D=Average

Figure 8 Influences of interaction factors on droplet coverage at 250 cm height

Above all, as the influence of main factors on droplet coverage rate changed with heights of pole, it is necessary to adjust operating parameters of sprayer at different heights in order to satisfy the desired prevention and cure effects.

4 Approximate models of factors

From the previous analysis, it is necessary to adjust and optimize operating parameters of sprayer at different heights in order to realize optimal spraying effects. However, because of complicated atomization principles, it is unrealistic to establish a completely accurate model of spraying performance, equivalent model with reliable accuracy is enough.

In the optimization design, approximate model approximates the relationships between input and output variables through using mathematics, which is able to solve two kinds of problems in practical projects: 1) unable to establish explicit mathematical optimization model because of complicated structure; 2) established model is too complex to solve. The basic thought of approximate model is to establish a model which has enough accuracy and simple calculation based on limited test data. There are some common approximate models, such as RSM model, Kriging model, Multivariate Adaptive Regression Spline (MARS) model, and Radial Basis Function (RBF) Neural Network model (Han et al., 2012).

4.1 RSM model

Quadratic regression fitting models were established through software Design-Expert 8.0.6 based on analysis results of response surface method, which were able to explain the relationships between droplet coverage rate and spraying parameters when the distance between center line of sprayer and sampling poles was 2 m. By guaranteeing the models are significant and unfit terms are insignificant as premises, insignificant terms were rejected according to P value in Table 3, RSM models were figured out and presented as Equations (1)-(3):

$$R_1 = 5.49 + 0.60 \times A - 0.29 \times B + 0.046 \times C + 0.55 \times D - 0.54 \times AB - 0.33 \times BC + 0.50 \times BD - 0.29 \times CD - 0.85 \times A^2 + 0.78 \times C^2 \quad (1)$$

$$R_2 = 4.64 + 1.24 \times A - 0.088 \times B + 0.39 \times C + 0.16 \times D + 0.37 \times BC - 1.32 \times A^2 - 0.29 \times B^2 \quad (2)$$

$$R_3 = 3.23 + 0.81 \times A - 0.16 \times B + 0.21 \times C + 0.082 \times D - 0.38 \times BD - 0.27 \times CD - 1.09 \times A^2 - 0.62 \times B^2 \quad (3)$$

where, A is angle of guide plate, °; B is air velocity of fan, m/s; C is pressure of pump, MPa; D is length of guide plate, cm; R_1, R_2, R_3 respectively represents droplet coverage rate at heights of 150, 200 and 250 cm, and unit of them is %.

Determination coefficients R^2 of optimized models were respectively calculated as 91.31%, 92.49%, 90.61% at the heights of 150, 200 and 250 cm, which indicated that the models could fit about more than 90% response variables with high correlation and low error between predicted and test values. Furthermore, maximums of droplet coverage rate at different heights were set as object function, and variation range of its variables were the same as Table 1. Based on RSM models, optimization spraying parameters at different heights were calculated out and presented in Table 4.

Table 4 Predicted value of RSM model

Height, cm	A: Angle of guide plate, °	B: Air velocity of fan, m/s	C:Pressure of pump, MPa	D: Length of guide plate, cm	Droplet coverage rate, %
150	39.97	24.95	0.51	88	57.04
200	45.57	20.23	1.47	88	29.81
250	44.88	20.73	1.49	38	15.40

4.2 RBF Neural Network model

RBF Neural Network is a local approximate network with three layers. The first layer is input layer consisting of sensing units, and is used to connect input variables with neural network. The second layer is hidden layer used to translating input space to hidden space as non-linear transformations. It should be pointed out that RBF is usually a non-negative and non-linear function, which is radial symmetry and attenuation around central point. The third layer is linear output layer used to output response values of corresponding input variables. RBF Neural Network has many advantages such as simple structure, fast convergence rate of learning and could approximate any continuous functions with arbitrary precision (Shi, 2009; Wang et al., 2015).

As parameters optimization of improved air-assisted orchard sprayer is a multi-objective optimization problem, multi-objective optimization algorithm was adopted to calculate the final results. RBF Neural Network models were established through software Isight according to data in Table 3, and approximate models of droplet coverage rate at different heights were figured out and presented as Equation (4):

$$\begin{cases} \max R_1' = f_1(\mathrm{A,B,C,D}) \\ \max R_2' = f_2(\mathrm{A,B,C,D}) \\ \max R_3' = f_3(\mathrm{A,B,C,D}) \end{cases} \tag{4}$$

where A, B, C, D are same as Equations (1)-(3); R'_1, R'_2, R'_3 respectively represents droplet coverage rate at heights of 150, 200 and 250 cm, and units of them are %.

Determination coefficients R^2 of optimized models were respectively calculated as 95.76%, 97.19%, and 97.54% at heights of 150, 200 and 250 cm, which indicated that the models could fit about more than 95% response variables. It is easily to find that determination coefficients of RBF Neural Network models are all higher than RSM models, because RSM is limited at quadratic polynomial which has bounded capabilities of fitting test data. However, RBF Neural Network adapts global non-linear fitting which has higher precision.

Furthermore, maximums of droplet coverage rate at different heights were set as object function, and variation range of its variables were same as Table 1. Using software through NSGA-II multi-objective genetic algorithm, population size was set as 10, evolutional generation was set as 20, cross-over rate was set as 0.4, and mutation probability was set as 0.02, optimization spraying parameters at different heights were calculated out and presented in Table 5.

Table 5 Predicted value of RBF neural network model

Height, cm	A: Angle of guide plate, °	B: Air velocity of fan, m/s	C: Pressure of pump, MPa	D: Length of guide plate, cm	Droplet coverage rate, %
150	32.82	24.48	0.50	88	57.06
200	44.64	21.42	1.50	38	29.67
250	43.20	21.72	1.49	38	15.58

4.3 Verification of models

To verify the precision of modes, tests were repeated for three times based on optimized operation parameters presented in Tables 4 and 5. Averages of droplet coverage rate at different heights were selected as final results presented in Table 6. According to Table 6, both of RSM model and RBF neural network model are able to fit the droplet coverage rate at different sample heights. Meanwhile, the precision of RBF Neural Network is better than RSM, which causes by restriction fitting ability of quadratic regression RSM model. Therefore, RBF Neural Network model was selected as reference to optimize parameters of sprayer.

Table 6 Comparison of predicted and test value with different models

Height, cm	RSM Model			RBFNN Model		
	Predicted value, %	Test value, %	Relative error, %	Predicted value, %	Test value, %	Relative error, %
150	57.04	60.58	6.2	57.06	55.06	3.5
200	29.81	27.16	8.9	29.67	28.13	5.2
250	15.40	17.22	11.8	15.58	17.01	9.2

5 Conclusions

(1) Based on RSM, length and angle of guide plate, air velocity of air outlet, and pressure of pump were opted as influence factors. In addition, droplet coverage rate was taken as response index of spraying. And orthogonal tests with mixed levels based on Box-Behnken method were designed and carried out. Furthermore, influences of the improved sprayer operating parameters on spraying effects were found out as follow: in the vertical plane which was 200 cm away from the center line of axial-flow fan, at height of 150 cm, the sequence of factors according to significant degree of influences on droplet coverage rate was length of guide plate, angle of guide plate, air velocity of fan, and pressure of pump; at height of 200 cm, the sequence was angle of guide plate, pressure of pump, length of guide plate, and air velocity of fan; at height of 250 cm, the sequence was angle of guide plate, pressure of pump, air velocity of fan, and length of guide plate.

(2) RSM model and RBF Neural Network model were

respectively adopted to approximate the relationships and establish the approximate models between experimental factors and experimental data. In verification tests, at height of 150 cm, droplet coverage rate and forecast error were 55.06% and 3.5%; at height of 200 cm, they were 28.13% and 5.2%; at height of 250 cm, they were 17.01% and 9.2%. The results showed that both of the two approximate models are able to fit the droplet coverage rate at different sample heights. Meanwhile, the model of RBF Neural Network was proved better, which causes by restriction fitting ability of quadratic regression RSM model.

(3) Based on RBF Neural Network model, optimization operating parameters of improved air-assisted orchard sprayer were figured out as follow: at height of 150 cm, length of guide plate was 88 cm, angle of guide plate was 32.82°, air velocity of air outlet was 24.48 m/s, and pressure of pump was 0.5 MPa; at height of 200 cm, length of guide plate was 38 cm, angle of guide plate was 44.64°, air velocity of air outlet was 21.42 m/s, and pressure of pump was 1.5 MPa; at height of 250 cm, length of guide plate was 88 cm, angle of guide plate was 43.20°, air velocity of air outlet was 21.72 m/s, and pressure of pump was 1.49 MPa. The results indicated that it was necessary to adjust operating parameters of sprayer at different heights in order to realize optimal spraying effects for canopies at different heights.

Acknowledgements

This work was partially financed by the National Key Research and Development Plan: High Efficient Ground and Aerial Spraying Technology and Intelligent Equipment (Grant No. 2016YFD0200700).

[References]

[1] Endalew, A. M., C. Debaer, N. Rutten, J. Vercammen, M. A. Delele, H. Ramon, B. M. Nicolaï, and P. Verboven. 2010. A new integrated CFD modelling approach towards air-assisted orchard spraying. Part I. Model development and effect of wind speed and direction on sprayer airflow. *Computers and Electronics in Agriculture*, 71(2): 128–136.

[2] Gu, J. B., W. M. Ding, W. Qiu, and C. D. Sun. 2014. Current research situation and development trend of equipment and technology for orchard spraying. *Journal of Fruit Science*, 31(6): 1154–1157.

[3] Han, D., and J. R. Zheng. 2012. A Survey of metamodeling techniques in engineering optimization. *Journal of East China University of Science and Technology: Natural Science Edition*, 38(6): 762–768.

[4] Jiang, H. H., P. Bai, L. M. Liu, X. F. Dong, J. L. Song, and X. H. Zhang. 2016. Caterpillar self-propelled and air-assisted orchard sprayer with automatic target spray system. *Transactions of the Chinese Society for Agricultural Machinery*, 47(S1): 189–195. (In Chinese with English abstract)

[5] Qi, L. J., Y. Q. Zhao, J. Wang, R. H. Ji, and L. Mang. 2010. CFD simulation and experiment verification of droplet dispersion of air-assisted orchard sprayer. *Transactions of the Chinese Society for Agricultural Machinery*, 41(2): 62–67. (In Chinese with English abstract)

[6] Qiu, W., J. B. Gu, W. M. Ding, X. L. Lv, C. D. Sun, and J. Lu. 2015. Experiment on control effect of different pesticide concentration using air-assisted sprayer. *Transactions of the Chinese Society for Agricultural Machinery*, 46(1): 94–99. (In Chinese with English abstract)

[7] Salcedo, R., R. Granell, G. Palau, A. Vallet, C. Garcerá, P. Chueca, and E. Moltó. 2015. Design and validation of a 2D CFD model of the airflow produced by an airblast sprayer during pesticide treatments of citrus. *Computers and Electronics in Agriculture*, 116(C): 150–161.

[8] Shi, Z. Z. 2009. Neural Network. *Beijing: Higher Education Press*.

[9] Song, S. R., T. S. Hong, D. Z. Sun, Y. Q. Zhu, and C. Luo. 2011. Effect of fan power supply frequency on deposition of air-assisted sprayer. *Transactions of the Chinese Society of Agricultural Engineering*, 27(1): 153–159. (In Chinese with English abstract)

[10] Song, S. R., H. B. Xia, H. S. Liu, T. S. Hong, D. Z. Sun, and Y. H. Lu. 2013. Numerical simulation and experiment of structural optimization for air-blast sprayer. *Transactions of the Chinese Society for Agricultural Machinery*, 44(6): 73–78, 55. (In Chinese with English abstract).

[11] Sun, C. D., W. Qiu, W. M. Ding, and J. B. Gu. 2015. Parameter optimization and experiment of air-assisted spraying on pear trees. *Transactions of the Chinese Society of Agricultural Engineering*, 31(24): 30–38. (In Chinese with English abstract)

[12] Wang, J. X., L. J. Qi, and Q. J. Xia. 2015. CFD simulation and validation of trajectory and deposition behavior of droplets around target affected by air flow field in greenhouse. *Transactions of the Chinese Society of Agricultural Engineering*, 31(11): 46–53. (In Chinese with English abstract)

[13] Wang, Z. T., Y. H. Zhang, Q. M. Dong, X. Y. Wang, and J. L.

Wen. 2015. Experiment of wind-blowing electrostatically charged spray. *Journal of Jiangsu University: Natural Science Edition*, 36(4): 425–430. (In Chinese with English abstract)

[14] Wang, W. J., J. Pei, S. Q. Yuan, J. F. Zhang, C. Z. Xu, and F. Zhang. 2015. Optimization of impeller meridional shape based on radial basis Neural Network. *Transactions of the Chinese Society of Agricultural Engineering*, 46(6): 78–83. (In Chinese with English abstract)

[15] Zhang, X. H., Z. Y. Jiang, G. Q. Fan, and L. L. Cao. 2014. Self-propelled crawler directional air-blowing orchard sprayer. *Transactions of the Chinese Society of Agricultural Engineering*, 45(8): 117–122, 247. (In Chinese with English abstract)

[16] Zhang, X. H., L. J. Wang, C. L. Hou, Y. L. Li, and H. M. Feng. 2016. Development and experiment of air-assisted vineyard sprayer. *Journal of Chinese Agricultural Mechanization*, 37(7): 57–61, 74. (In Chinese with English abstract)

[17] Zhou, L. F., L. Zhang, X. Y. Xue, W. M. Ding, Z. Sun, Q. Q. Zhou, and L. F. Cui. 2016. Design and experiment of 3WQ-400 double air-assisted electrostatic orchard sprayer. *Transactions of the Chinese Society of Agricultural Engineering*, 32(16): 45–53. (In Chinese with English abstract)

[18] Zhou, L. F., X. M. Fu, W. M. Ding, S. M. Ding, J. Chen, and Z. J. Chen. 2015. Design and experiment of combined disc air-assisted orchard sprayer. *Transactions of the Chinese Society of Agricultural Engineering*, 31(10): 64–71. (In Chinese with English abstract)